ISSN 0965-545X, Polymer Science, Ser. A, 2007, Vol. 49, No. 7, pp. 816–827. © Pleiades Publishing, Ltd., 2007.
Original Russian Text © A.L. Volynskii, T.E. Grokhovskaya, A.I. Kulebyakina, A.V. Bol'shakova, N.F. Bakeev, 2007, published in Vysokomolekulyarnye Soedineniya, Ser. A, 2007, Vol. 49, No. 7, pp. 1224–1238.

Visualization of Structural Rearrangements during Annealing of Solvent-Crazed Poly(ethylene terephthalate)[1]

A. L. Volynskii, T. E. Grokhovskaya, A. I. Kulebyakina, A. V. Bol'shakova, and N. F. Bakeev

Faculty of Chemistry, Moscow State University, Leninskie gory, Moscow, 119992 Russia
e-mail: volynskii@mail.ru

Received September 13, 2006;
Revised Manuscript Received February 12, 2007

Abstract—A direct microscopic procedure is used for studying structural rearrangements during the annealing of PET samples after solvent crazing. Even at room temperature, solvent-crazed PET samples experience shrinkage which is provided by processes taking place in crazes. This shrinkage is observed at temperatures up to the glass transition temperature of PET and proceeds via drawing together of crack walls. Once the glass transition temperature is attained during annealing, the spontaneous self-elongation of the polymer sample occurs. The mechanism of this phenomenon is proposed. The low-temperature shrinkage of the polymer sample is related to the entropy contraction of highly dispersed material in crazes that has a lower glass transition temperature than that of the bulk polymer. This shrinkage cannot be complete, owing to crystallization of the oriented polymer in the volume of the crazes. As a result of crystallization, the oriented and crystallized polymer in the crazes coexists with the regions of the unoriented initial PET. As the annealing temperature approaches the glass transition temperature of the bulk PET, its strain-induced crystallization takes place. As a result, the regions of the unoriented polymer between crazes are elongated along the direction of tensile drawing and the sample experiences contraction in the normal direction.

DOI: 10.1134/S0965545X07070073

INTRODUCTION

Determing the mechanism of deformation of amorphous glassy polymers is a challenging task of modern materials science. The solution of this problem is primarily limited by the absence of any direct experimental methods for studying structural rearrangements in polymers. In recent years, a new microscopic procedure has been proposed [1–4]. This procedure allows one to gain direct information concerning structural rearrangements. The use of this procedure made it possible to obtain new data on the mechanism of the deformation of amorphous polymers below [5] and above [6] the glass transition temperature. In particular, as was found in [6, 7], the annealing of PET samples after their orientation above the glass transition temperature is accompanied by their elongation along the direction of preliminary tensile drawing. This phenomenon is referred to as a spontaneous self-elongation (SSE). In the above-cited works, the SSE phenomenon is shielded by the shrinkage of a polymer, which likewise takes place during annealing. In this case, the overall length of the samples after annealing appears to be smaller than their initial size; however, the process of self-elongation has been revealed and visualized by the use of the proposed microscopic procedure.

It is of importance that the SSE phenomenon during the annealing of the solvent-crazed PET samples was discovered long ago [8, 9]. In this case, the intensity of self-elongation is so high that the resultant dimensions of the samples after annealing appear to be much higher than those before annealing. Crazed polymers are characterized by a rather complex structure, which contains coexisting regions of a crazed material and an undeformed polymer. Owing to the presence of above alternate regions, interpretation of the thermomechanical behavior of the material becomes much more complicated; therefore, the detailed mechanism behind the temperature-induced changes in the dimensions of the solvent-crazed PET samples remains unclear.

The objective of this study concerns the use of the direct microscopic procedure [1–4] for studying structural rearrangements taking place in the solvent-crazed PET samples during annealing.

EXPERIMENTAL

In this study, we examined commercial films of amorphous PET with a thickness of 100 μm. Changes in the geometrical dimensions of the test samples during annealing was studied according to the following procedure. The sample was suspended in a narrow gap between two glasses and placed into a thermostated cell; temperature-induced changes in the linear dimen-

[1] This work was supported by the Russian Foundation for Basic Research, project nos. 05-03-32538 and 06-03-08025-ofi.

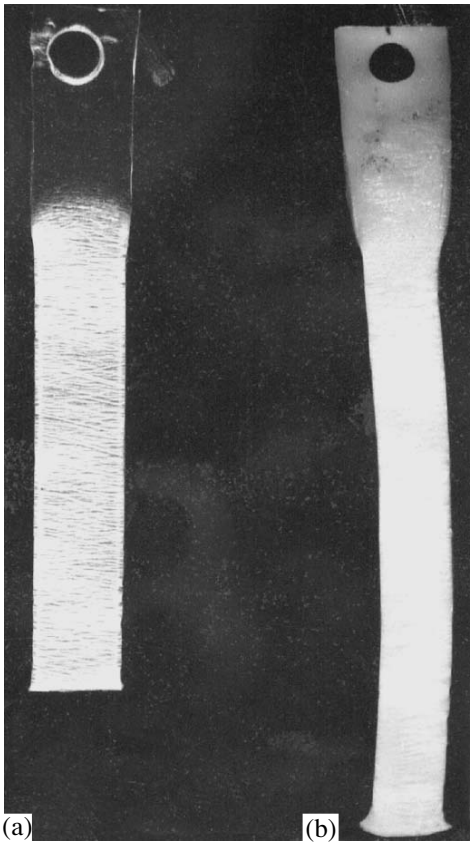

Fig. 1. Appearance of the solvent-crazed PET sample (a) before and (b) after annealing at 170°C.

sions of the samples were measured on a KM-6 cathetometer; and the corresponding temperature dependences were constructed. The current strain of the polymer sample during annealing was estimated as $\varepsilon = \Delta l/\Delta l' \times 100\%$, where Δl and $\Delta l'$ stand for changes in the linear dimensions of the sample during heating and tensile drawing, respectively. The samples oriented via necking were prepared by tensile drawing in air at a strain rate of 10 mm/min at room temperature. Other test samples were prepared by tensile drawing in the presence of ethanol via hand-operating clamps.

To visualize structural rearrangements taking place in the solvent-crazed PET samples during annealing, their surface (before annealing) was decorated with a thin (10 nm) platinum coating via the method of ionic plasma deposition. The morphology of the strained samples was examined on a Hitachi S-520 scanning electron microscope. The samples for electron-microscopic observations were prepared by the method of brittle fracture at liquid nitrogen temperature. Optical microscopic studies were conducted on an Opton-3 light microscope.

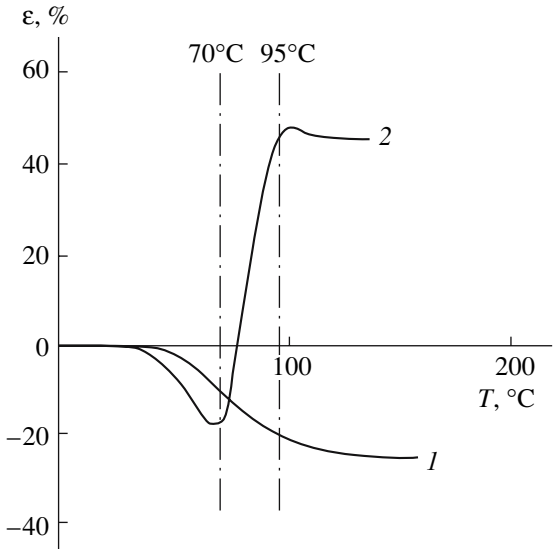

Fig. 2. Thermomechanical curves of the PET samples (*1*) after their tensile drawing in air via necking and (*2*) after stretching in ethanol by a tensile strain of 50%.

RESULTS AND DISCUSSION

Figure 1 presents the visual appearance of the two solvent-crazed PET samples after their stretching in ethanol by a tensile strain of 50%. Under the above stretching conditions, the polymer sample is deformed via nucleation and development of microscopic regions that contain highly oriented fibrillar material (crazes). When the solvent-crazed sample with fixed dimensions is dried in the hand-operated clamps and the mechanical stresses are released, the resultant linear dimensions of the sample remain unchanged. This sample is shown in Fig. 1a. After annealing at 170°C, evident changes in the appearance of the sample can be observed with the naked eye (Fig. 1b). The uncrazed part of the sample becomes milky white and opaque owing to occurrence of the so-called cold crystallization. Furthermore, one can clearly distinguish that the linear dimensions of the sample along the direction of preliminary tensile drawing are increased, whereas dimensions in the perpendicular direction are decreased. The evidence presented in Fig. 1 vividly illustrates the occurrence of the SSE phenomenon in the solvent-crazed PET sample during annealing.

Let us mention that the thermomechanical response of the solvent-crazed PET samples during annealing shows a rather complex character. Figure 2 presents the corresponding thermomechanical curves of the PET samples oriented under different stretching conditions. One sample (curve *1*) is stretched in air at room temperature via necking. As is expected, the annealing of this sample is accompanied by a marked shrinkage that appears to be incomplete owing to cold crystallization. At the same time, the solvent-crazed PET sample pre-

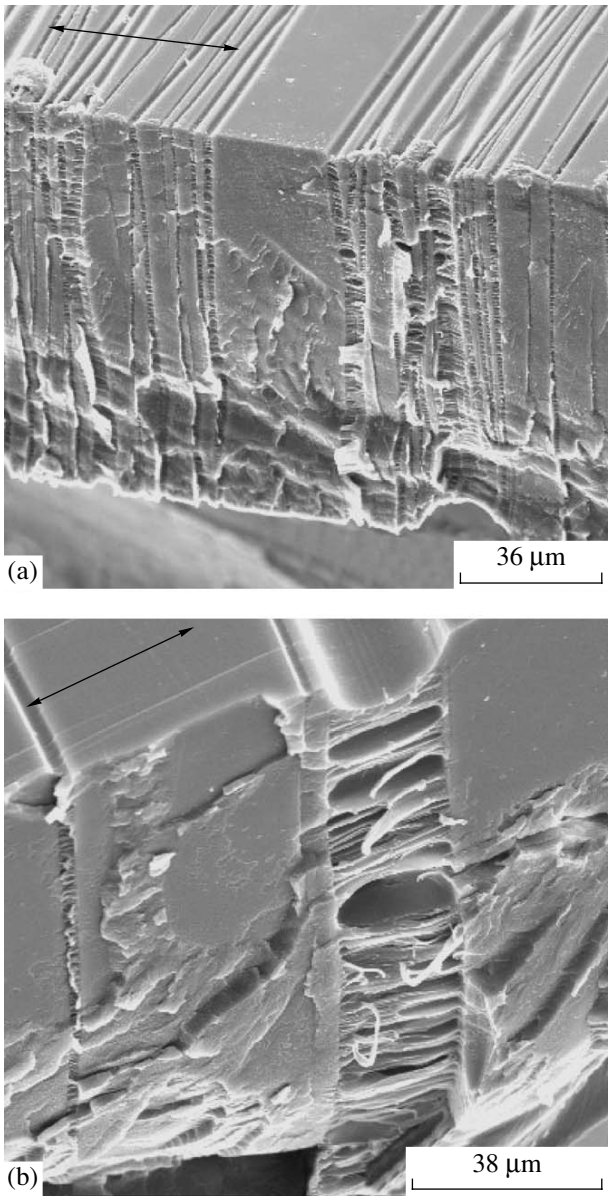

Fig. 3. SEM images of the solvent-crazed PET sample stretched in ethanol by 50%. Hereinafter, arrows show the direction of tensile drawing. Comments are given in text.

pared by stretching in ethanol via the mechanism of solvent crazing is characterized by an extremely unorthodox thermomechanical behavior (Fig. 2, curve *2*). After the stage of low-temperature shrinkage, when the annealing temperature approaches the glass transition temperature of PET, the linear dimensions of the polymer sample are increased along the direction of preliminary tensile drawing (the SSE phenomenon). It is important that the SSE phenomenon takes place in a rather narrow temperature interval from 65–70 to 95°C. Questions concerning the mechanism of the phenomena taking place during the temperature-induced structural rearrangements in the solvent-crazed PET ariss. First, what is the cause of the shrinkage of the polymer sample at temperatures below the glass transition temperature? Second, why, in the temperature region of glass transition, is this shrinkage replaced with the spontaneous self-elongation of polymer and which factors control the temperature limits of the above phenomena? Third, what are the driving forces providing low-temperature shrinkage and self-elongation?

With consideration for the complex structure of the solvent-crazed polymer (unoriented regions alternate with crazes with the fibrillar–porous structure), it seems necessary to ascertain the way in which the complex structure of the solvent-crazed polymer controls changes in the geometrical dimensions.

The electronic microscopic image of the solvent-crazed PET film after its stretching by a tensile strain of 50% in the presence of adsorptionally active solvent (ethanol) is shown in Fig. 3. The above SEM images clearly show the surface and inner fractured structure of the sample. As is seen, the tensile drawing of PET is accompanied by the development of crazes that grow in the direction perpendicular to the direction of the applied stress and the grown crazes propagate across the entire cross-sectional area of the sample (Fig. 3a). At the surface of each craze, craze fibrils that are typical of the craze structure coalescence and form a monolithic top film that isolates the inner craze structure (Fig. 3b). Note that, as a result of removal of an active liquid from the craze volume, the above thin film is seen to be saddle-shaped. Nevertheless, within the craze volume, except for the surface, craze fibrils formed by the oriented macromolecules appear to be disintegrated and form a typical fibrillar–porous structure. As follows from Fig. 3, the surface of the above thin films on the top of each craze, as well as the surface of the regions of the initial polymer between crazes, has a smooth and flat relief. The above morphological features of the solvent-crazed PET samples have been found and described in detail in our earlier publications [10, 11].

Figure 4 presents the SEM images of the PET sample (its structure is shown in Fig. 3) after its annealing at 170°C. As is seen, the annealing of the solvent-crazed polymer that is accompanied by the low-temperature shrinkage and subsequent SSE (Fig. 2) likewise leads to marked structural changes in the sample. On the surface of the solvent-crazed films, the edges of crazes become more smooth, flat, and oval. The inner structure of crazes experiences dramatic changes as well. As a result of annealing, the formed fibrillar–porous structure of crazes appears to be less regular. Fibrils become thicker, and the craze structure contains less microvoids. Nevertheless, the surface of the sample (as the surface of crazes and regions between them) remains flat and smooth.

The above experimental evidence illustrates the structure of solvent-crazed PET samples before (Fig. 3) and after annealing (Fig. 4). However, microscopic

observations do not allow one to characterize the complex structural rearrangements taking place during annealing of the solvent-crazed PET. Indeed, changes in the geometrical dimensions, high shrinkage, and subsequent elongation should be accompanied by a marked inner mass transfer under the action of stored stresses. Using the above results, one can hardly characterize the whole process and demonstrate how the structure of the solvent-crazed polymer shown in Fig. 3 is transformed into the structure shown in Fig. 4 in the course of annealing. Evidently, without knowledge of the detailed pattern of structural rearrangements taking place during annealing of the solvent-crazed PET samples, it is impossible to offer any adequate description of the observed phenomena.

In our recent studies, we proposed a new universal procedure for the visualization of structural changes during deformation of solid polymers [1–4]. In this case, the procedure for the preparation of the test samples is rather simple and involves the following steps. Prior to tensile drawing or shrinkage of the polymer sample, its surface is decorated with a thin (10–15 nm) metallic coating. As a result of subsequent tensile drawing of the polymer support, the deposited coating experiences certain structural rearrangements that are directly related to processes taking place in the polymer sample. Using direct electron microscopic observations, one can easily follow those structural rearrangements that offer some information concerning the mechanism of deformation of the polymer support.

To use the above approach, the surface of the PET sample, whose structure is shown in Fig. 3, was decorated with a thin (10 nm) platinum coating; then, the coated sample was annealed at 170°C. Figure 5a shows the structure of the as-prepared sample. The deposition of a thin metallic coating onto the surface of the solvent-crazed polymer before annealing makes it possible to reveal marked changes in its morphology (cf. Figs. 3 and 5a). First, the fragments of the undeformed polymer located between crazes acquire a regular wavy relief and the folds of this relief are oriented along the direction of tensile drawing. Second, the surface of a thin film on the top of crazes likewise appears to be covered with a regular wavy microrelief (Fig. 5b). At high magnifications, the corresponding SEM images (Fig. 5c) clearly show that the folds in the above regions are oriented along and perpendicular to the direction of stretching. It is important that the regular microrelief on the top of the fragments between crazes has a fixed period of ≈2 μm. As follows from Fig. 5d, at the boundary between a craze and unoriented polymer, this regular microrelief is transformed into another regular microrelief but with a much smaller period (≈0.4 μm).

As was mentioned above, changes in the geometrical dimensions of the solvent-crazed PET upon annealing are provided by the transfer of a polymer material into the volume and from the volume of the samples as their surface area is changed. A comparison of Figs. 3 and 4 lead us to conclude that this mass transfer proceeds via diffusion of the polymer material, so that the relief of the formed surface remains smooth. The preliminary deposition of the metallic coating onto the surface of the solvent-crazed polymer allows one to reveal the location and character of the localized regions of the above mass transfer upon annealing because the metallic coating is incompatible with polymer and cannot diffuse into the polymer volume. As a result, the coating acquires a certain microrelief that bears information concerning the mechanism of structural rearrangements in the polymer support [12, 13].

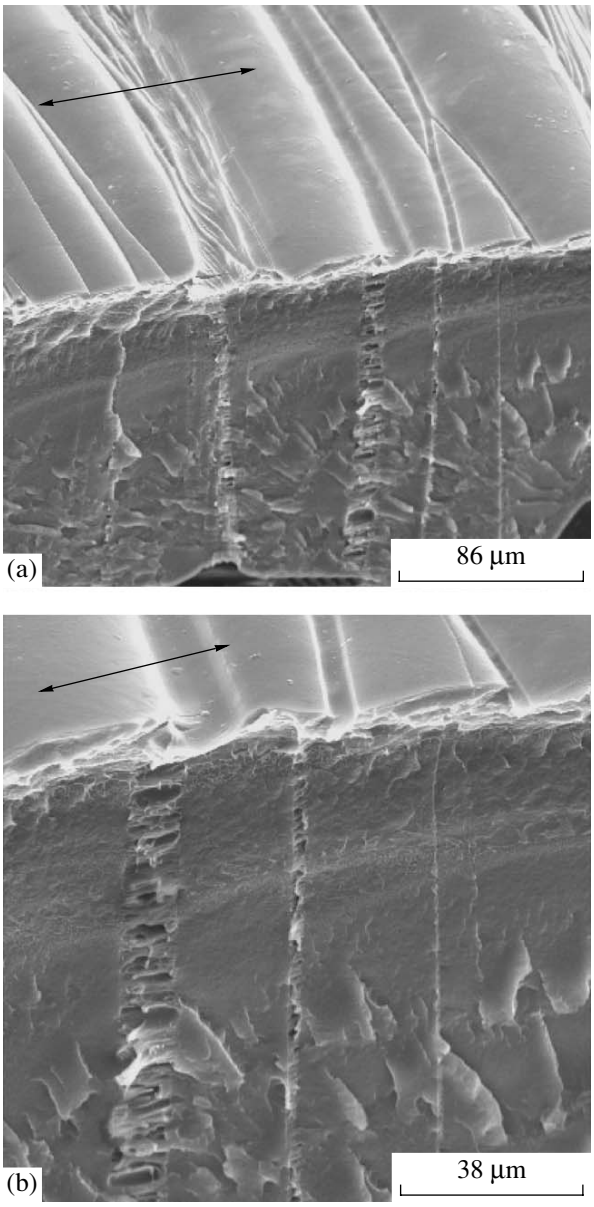

Fig. 4. SEM images of the solvent-crazed PET sample stretched in ethanol by 50% after its annealing at 170°C. Comments are given in text.

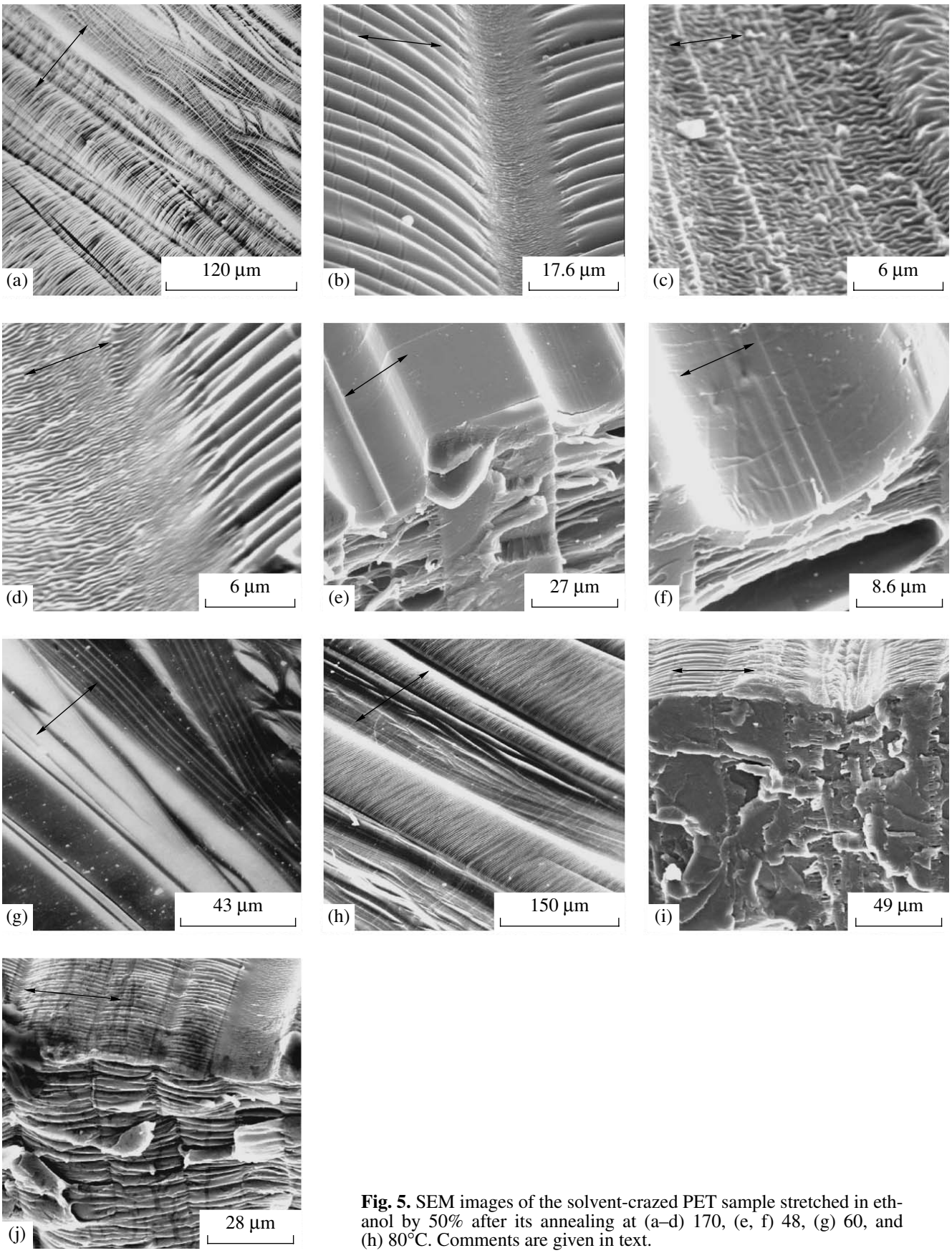

Fig. 5. SEM images of the solvent-crazed PET sample stretched in ethanol by 50% after its annealing at (a–d) 170, (e, f) 48, (g) 60, and (h) 80°C. Comments are given in text.

Figures 5e and 5f show the SEM images of the solvent-crazed PET sample with the deposited metallic coating after annealing at 48°C. At this temperature, the sample experiences only small shrinkage (Fig. 2) and, at first sight, no marked morphological changes are expected. Indeed, the boundary between the crazes and undeformed polymer on the surface of the sample is still sharp and the surface of the regions of the undeformed polymer and thin films on the top of crazes remains smooth (Fig. 5e). However, at high magnifications, it is possible to distinguish on the surface of the films on top of crazes thin rectilinear folds that pass through the central part of the crazes (Fig. 5f).

When the annealing temperature is increased above 60°C, the above folds become more pronounced. At the same time, the surface of polymer fragments between crazes remains smooth (Fig. 5g). The above folds should be inevitably formed in the thin metallic coating deposited onto the surface of the solvent-crazed PET samples when craze walls come closer to each other. It should be noted that, at low annealing temperatures (below 60°C), the surface of regions between crazes remains smooth and its relief does not change. This observation implies that this part of polymer does not contribute to changes in the dimensions of the sample and plays no role in the observed macroscopic shrinkage. This circumstance suggests that the low-temperature shrinkage of the polymer is totally provided by the processes taking place in the volume of the formed crazes.

As a result of annealing at 80°C, the structural features on the polymer surface are similar to those as observed upon high-temperature annealing (Fig. 5h). One can see a well-pronounced wavy relief on the surface of polymer regions located between crazes. At the same time, on the surface of crazes, another regular microrelief with a smaller period is formed; this microrelief coexists with rectilinear folds that are oriented perpendicular to the direction of tensile drawing.

As the annealing temperature is increased up to 170°C, no marked morphological changes in the solvent-crazed PET samples are observed. Figure 5i clearly shows that the entire surface of the polymer fragments between crazes is covered with a regular wavy microrelief. This experimental fact indicates compression of the above regions in the direction perpendicular to the axis of tensile drawing. However, this relief is absent on the fractured surface of the sample. However, one cannot conclude that the transverse contraction of the above regions in the volume of the polymer sample does not take place. Remember that the sample shown in Fig. 5i was prepared according to the following procedure. The surface of the solvent-crazed PET sample was covered with a thin metallic coating, and the as-coated sample was subjected to annealing. Then, the sample was fractured, and the fractured surface was examined by direct microscopic observations. With consideration for the fact that, prior to annealing, the fractured surface has no metallic coating, one cannot visualize the consequences of mass transfer in these regions. However, if the test samples are prepared in a somewhat different way, processes taking place in the volume of the polymer sample can be visualized. Figure 5j shows the SEM image of the sample with its own temperature–stress prehistory that is similar to that of the sample shown in Fig. 5i. The difference between the samples is the following. The polymer sample was coated with a thin metallic layer not before but after fracture in liquid nitrogen; then, the sample was annealed under the same temperature regime as the sample shown in Fig. 5i. In this case, one can clearly observe formation of a regular relief not only on the surface of the sample but also at its fractured surface in the bulk. This fact indicates that the SSE process takes place in the entire volume of the unoriented part of the PET sample located between crazes.

Let us describe the pattern of structural rearrangements during annealing of the solvent-crazed PET samples on the basis of the above experimental evidence. An analysis of the SEM images shown in Figs. 5e, 5f, and 5g suggests that the shrinkage of the solvent-crazed PET below the glass transition temperature is provided by processes in the volume of crazes. Let us emphasize that, in this case, shrinkage takes place at temperatures well below the glass transition temperature of the bulk PET (Fig. 2). This unusual structural-mechanical and, in particular, thermomechanical behavior of solvent-crazed polymers was observed earlier.

There are many indications supporting the conclusion that the properties of solvent-crazed polymers are appreciably different from the properties of traditional oriented polymers [14]. This observation was first mentioned in [15]. As was shown in [15], the crazed PC is characterized by a lower elastic modulus and a higher reversible deformation as compared with the corresponding properties of the initial polymer. This unorthodox mechanical behavior of the crazed PC was explained in terms of the model of a craze as an open porous structure [16]. This assumption allows one to conclude that the molecular mobility in a craze is much higher than that in the polymer bulk owing to its proximity to the surface. The high molecular mobility of the polymer material in the craze was likewise confirmed by the data presented in [17]. As was shown in [17], the annealing of the crazed PS below T_g is accompanied not only by the closing-in movement of craze walls but also by polymer monolithization; in other words, healing of interfacial boundaries takes place. Therefore, one can conclude that craze fibrils are characterized by an exceptionally high molecular mobility.

Finally, one can cite the data reported in [18], where crazes were nucleated in thin PS films, their dimensions were fixed, and distances between fibrils and craze fibril diameter were measured with transmission electron microscopy. As was shown, under such experimental conditions, individual crazes tend to aggregate into

continuous bundles and thick secondary fibrils are formed. A distance between thick fibrils is higher than that between initial craze fibrils. These changes are accompanied by the coalescence (aggregation) of craze fibrils and, within 750 h, no individual fibrils are observed. Evidently, the observed structural rearrangements require a high mobility of molecular chains at much lower temperatures than T_g of bulk polymer.

The unusual mechanical properties of crazed polymers can be easily explained by the depression in the T_g of a highly dispersed oriented material of crazes. This behavior agrees with the experimental data obtained in the last decade [19, 20]. As was shown, the thin films and thin surface layers (tens and hundreds of nanometers) of bulk polymers are characterized by enhanced (as compared with bulk) large-scale molecular mobility, which is so intensive that the surface layers of bulk polymers have an appreciably lower T_g than that of the bulk polymer. Furthermore, according to [21, 22], all glassy polymers at room temperature are covered by a thin layer of a rubbery material.

As was calculated in [23], at a typical craze fibril diameter of 10 nm, each craze fibril contains no more than 10 chains. Therefore, all oriented macromolecules in craze fibrils are located in the surface layer and their glass transition temperature is lower than that of the bulk polymer. With due regard for the fact that the glass transition temperature depends on the remoteness of macromolecules from the surface [24–26], the fibrillar material in crazes is characterized by a lower glass transition temperature and a wider glass transition interval that is shifted to lower temperatures. Hence, the low-temperature shrinkage of solvent-crazed glassy polymers is provided by the entropy contraction of fibrils bridging the craze walls when their local glass transition temperature is attained. As follows from Figs. 5e–5g, the proposed microscopic procedure allows one to visualize the low-temperature shrinkage of PET that is related to processes taking place in crazes.

Let us consider the possible causes of the self-induced elongation of the solvent-crazed PET. It is worth mentioning (Fig. 2) that the low-temperature shrinkage of the solvent-crazed PET is virtually ceased in the temperature region of glass transition and that this process is replaced with SSE. This ceased shrinkage during annealing is likely explained by the onset of crystallization of the fibrillar craze material in the solvent-crazed PET samples. The behavior of PET oriented in air via necking (Fig. 2, curve *1*) appears to be virtually the same. The above phenomena are provided by the enhanced cold crystallization of PET due to orientation [27, 28].

The SEM images shown in Figs. 4 and 5h–5j allow one to suggest that the SSE of the solvent-crazed PET samples is related to the involvement of polymer regions located between crazes in the overall changes in geometrical dimensions of the test samples. Indeed, beginning from the annealing temperature of ≈70°C (when the T_g of bulk PET is attained), a regular wavy relief is formed on the surface of polymer regions located between crazes (Fig. 5h). The development of this relief indicates the compression of polymer support in the direction perpendicular to the axis of tensile drawing. At the same time, formation of the surface relief on the above polymer regions is accompanied by the development of a similar relief on the surface of crazes (Figs. 5b, 5c). However, the period of this relief appears to be an order of magnitude lower. This fact suggests, in particular, that the elastic modulus of the polymer at the top of crazes is much higher than the elastic modulus of the unoriented rubbery PET between crazes. The latter conclusion is not evident and demonstrates advantages of the proposed microscopic procedure [1–4].

Nevertheless, the question concerning the driving forces of SSE remains open. It shoule be emphasized that the SSE phenomenon is well known and was found during investigation of the structural mechanical behavior of some crystallizable polymers [29–31]. In particular, the SSE phenomenon was repeatedly observed for PET that was subjected to the action of various temperature–force factors. For example, the abnormal behavior of oriented PET fibers during annealing was reported in [32]. As was found, the shrinkage of the sample is 41% after its staying for 1 s at 220°C; within 20 min, shrinkage is as low as 34%. This situation corresponds to elongation by 14% with an increase in the duration of annealing. In contrast, according to [33], the oriented PET fibers increase their length with the annealing temperature. However, in both cases, the overall length of the samples after thermal treatment is likely to attest to the occurrence of shrinkage rather than elongation. In [34], the stress–strain optical properties of amorphous PET fibers were studied and certain annealing conditions were shown to induce elongation of the samples. This elongation was accompanied by an increase in birefringence. A marked increase in the length of the PET samples oriented at temperatures above T_g was reported in [6, 7, 35].

In most of the cited publications, the SSE phenomenon was described without any assumptions concerning its mechanism. In our opinion, the conclusions proposed by Bosley [36] seem to be justified when SSE is assumed to be provided by the orientation-induced crystallization of polymer. According to this model, a polymer should be slightly oriented before thermal treatment and its volume contains a certain amount of oriented nucleation sites of crystallization. When this system is subjected to annealing, crystallization commences at the above nucleation sites and leads to a situation when segments of amorphous chains experience an axial compression and the overall length of the sample increases.

A similar interpretation of the SSE phenomenon in the solvent-crazed polymers was presented in [37, 38]. As was shown, SSE can be attained not only via heating

of the crazed polymer but also via some other factors that are able to initiate crystallization: for example, swelling in solvents [37] or the radiation-induced temperature rise under high-energy electron irradiation [38]. In the cited works, the SSE phenomenon was rationalized by the strain-induced crystallization of PET in the transition regions between crazes and unoriented polymer.

The proposed microscopic procedure makes it possible to refine the pattern of structural rearrangements taking place during SSE. Our conclusion that the strain-induced crystallization commences at oriented nucleation sites located at the boundary between the craze and the unoriented polymer and then develops throughout the entire volume seems to be very important. Indeed, the data shown in Figs. 5i and 5j attest that unoriented polymer regions (not only boundary regions) are involved in the overall contraction. In other words, the SSE phenomenon is provided by the strain-crystallization taking place in the above regions of the solvent-crazed polymer. Hence, by increasing the tensile drawing of the solvent-crazed polymer or by decreasing the fraction of unoriented polymer regions in the solvent-crazed sample, one can reduce and even suppress the occurrence of the SSE phenomenon [9].

The key role of processes taking place in the oriented regions of the solvent-crazed PET is further confirmed by the data of light microscopy for the samples with a low craze density. To this end, PET film was stretched in an adsorptionally active environment by small tensile strains (3–5%) and dried with fixed dimensions. In this case, the number of the formed crazes in the polymer sample is small, and one can easily follow their evolution during annealing. Figure 6 shows light microscopic images illustrating the evolution of the same region in the solvent-crazed PET sample during annealing. As is seen, under the above experimental conditions, the number of formed crazes in the sample is low and they are located at high distances from each other (tens–hundreds of microns). Owing to their porous structure, crazes are clearly seen in the transparent PET film (Fig. 6a).

When this sample is heated to 70°C, crazes start to thicken (Fig. 6b). The thickness of each craze increases by a factor of 2–3. An analysis of the microscopic data allows one to conclude that the above thickening is related to the process of strain-induced crystallization. The crystallized PET is seen to be opaque and milky white, and this appearance produces an illusion of craze widening. In reality, this optical effect is related to the fact that crystallization proceeds via the advance of the front of crystallized (opaque) polymer inside the sample from the wall of each craze, at the boundary of which oriented craze material exists in the neighborhood with the unoriented bulk polymer. One can clearly see that crystallization proceeds along the direction of tensile drawing (in the normal direction to craze axis).

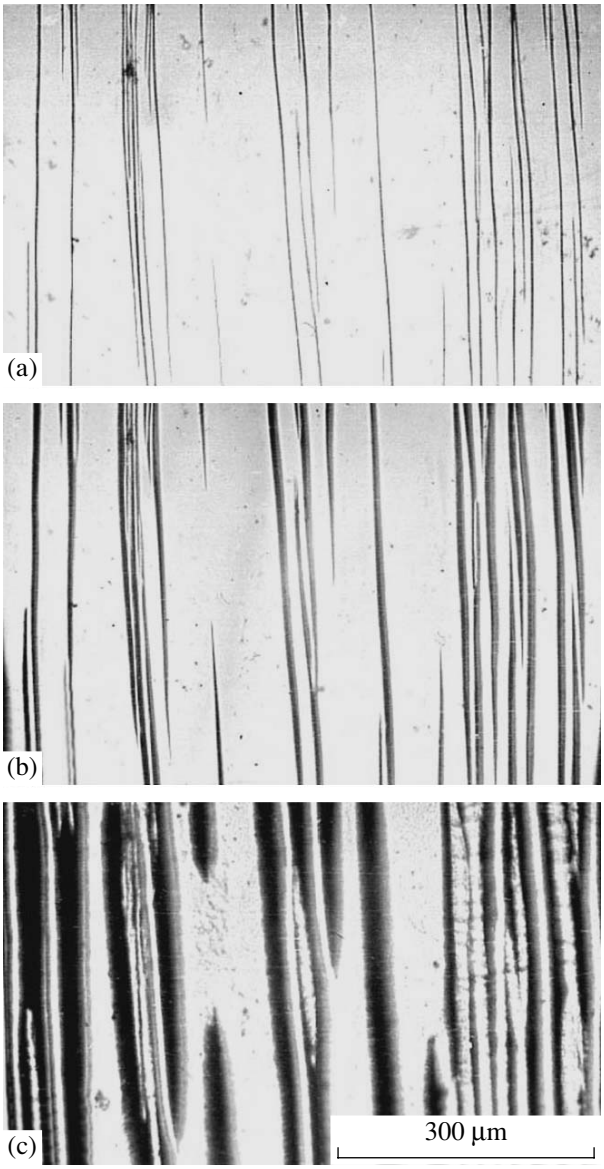

Fig. 6. Light microscopic images of the solvent-crazed PET samples (a) before and (b, c) after annealing at (b) 70 and (c) 95°C. The direction of stretching is horizontal.

The above process is completed at ≈95°C. At this temperature, the front of the strain-induced crystallization spans into the depth of the bulk polymer by many tens of microns. However, the crystallization process is ceased because a gradual disorientation of the polymer at the front on the boundary of amorphous bulk polymer and polymer crystallized in the oriented state is likely to occur. When the crystallization front moves by a long distance from the nucleation sites of strain-induced crystallization, material forgets them and crystallization is stopped. This behavior is related to the well-established fact that the crystallization of the amorphous PET is highly promoted by its molecular

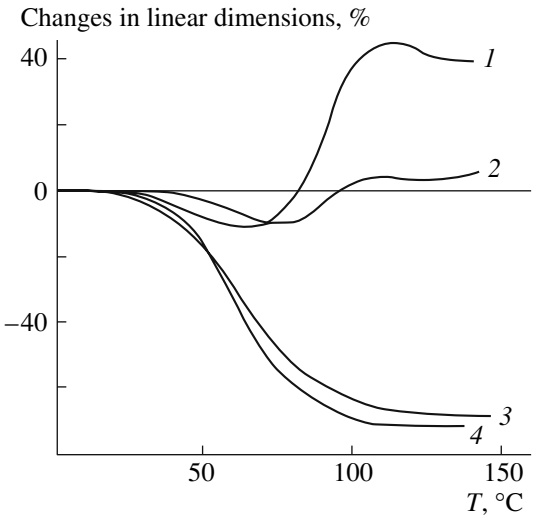

Fig. 7. Thermomechanical curves of (*1*) the amorphous PET sample (*2–4*) after its tensile drawing in ethanol by 50% and the solvent-crazed PET sample stretched in ethanol by 50% after preliminary annealing at (*2*) 100, (*3*) 110, and (*4*) 170°C.

orientation [27, 28]. At the same time, at 95°C, no crystallization of the unoriented PET is observed; as a result, the regions of PET crystallized in the oriented state are vividly seen against the background of the unoriented amorphous PET (Fig. 6c).

It is worth mentioning that, in regions with high density of crazes, different fronts of strain-induced crystallization approach each other; within the above regions, the polymer is totally transformed into the oriented crystalline state (Fig. 6c). Coming back to the structure of the PET samples that are able to experience SSE (Fig. 3), let us mention that the number of crazes in the above samples is much higher than that in the sample shown in Fig. 6. Evidently, in this case, distances between individual crazes are small (≈5–50 μm) and can be easily overpassed by the front of strain-induced crystallization. As a result, all bulk PET regions between crazes appear to be crystallized via the mechanism of strain-induced crystallization and this crystallization of bulk PET is the driving force of the SSE phenomenon.

Therefore, the general pattern of structural rearrangements during the annealing of solvent-crazed PET can be presented as follows. As was mentioned above, the annealing of the solvent-crazed PET sample is accompanied by its macroscopic shrinkage due to processes taking place within the craze volume. This process manifests itself as the development of folds along the axis of each craze. However, this shrinkage cannot be complete, owing to the strain-induced crystallization of the oriented polymer in the bulk of crazes. As a result of this crystallization, the oriented and crystallized crazed material appears to contact the blocks of the unoriented initial PET. In other words, oriented nucleation sites of crystallization have numerous contact points with the unoriented polymer. The crystallized crazed material is likely oriented along the direction of tensile drawing. This direction controls the course of the subsequent strain-induced crystallization in the bulk PET regions located between crazes. Evidently, as the annealing temperature approaches the glass transition temperature of bulk PET or, in other words, when the bulk polymer acquires a sufficient molecular mobility, the strain-induced crystallization commences. As a result, blocks of the unoriented polymer between crazes are elongated along the direction of tensile drawing. This process is accompanied by contraction of the sample in the normal direction. The overall contraction of the sample during SSE also entails the contraction of the regions occupied by crazes; as a result, their surface appears to be covered by a wavy regular surface relief.

According to the above speculations and the concept proposed by Bosley, the SSE phenomenon is provided by the processes of strain-induced crystallization in the blocks of unoriented PET. If these assumptions are valid, this explanation of the SSE phenomenon can be easily verified experimentally. Indeed, PET is readily crystallized upon its annealing above glass transition temperature and, as a result of this crystallization, its structure and properties are changed. In other words, there is a simple way to check the effect of the crystallization in unoriented PET fragments between crazes on the SSE phenomenon. To this end, prior to solvent crazing, PET samples were annealed at different temperatures, and thermomechanical properties of the solvent-crazed PET samples were studied. The obtained results are shown in Fig. 7. As is seen, preliminary annealing has a strong effect on the thermomechanical response of the solvent-crazed PET samples. In the case of the PET samples without preliminary annealing, SSE phenomenon is well pronounced, whereas its intensity decreases by several times when the samples are annealed at a temperature of 100°C. As the annealing temperature is increased further, SSE appears to be totally suppressed. At and above a temperature of preliminary annealing of 110°C, solvent-crazed PET samples experience only shrinkage.

Let us discuss how the preliminary annealing controls the morphology of the solvent-crazed samples and which structural rearrangements during annealing can be revealed via the proposed microscopic procedure [1–4]. Preliminary annealing of PET at 100°C does not entail any marked changes in the morphology of the solvent-crazed samples. As in earlier cases (cf. Figs. 3a, 3b, and 8a), tensile drawing is accompanied by the nucleation of crazes, which grow across the entire cross section of a polymer sample in the direction perpendicular to the direction of the applied tensile stress. The surface of each craze is topped by a thin film, which isolates its inner structure from the outer space. The surface of this saddle-shaped film remains smooth. The surface of undeformed polymer fragments between crazes likewise remains smooth. Within the volume of

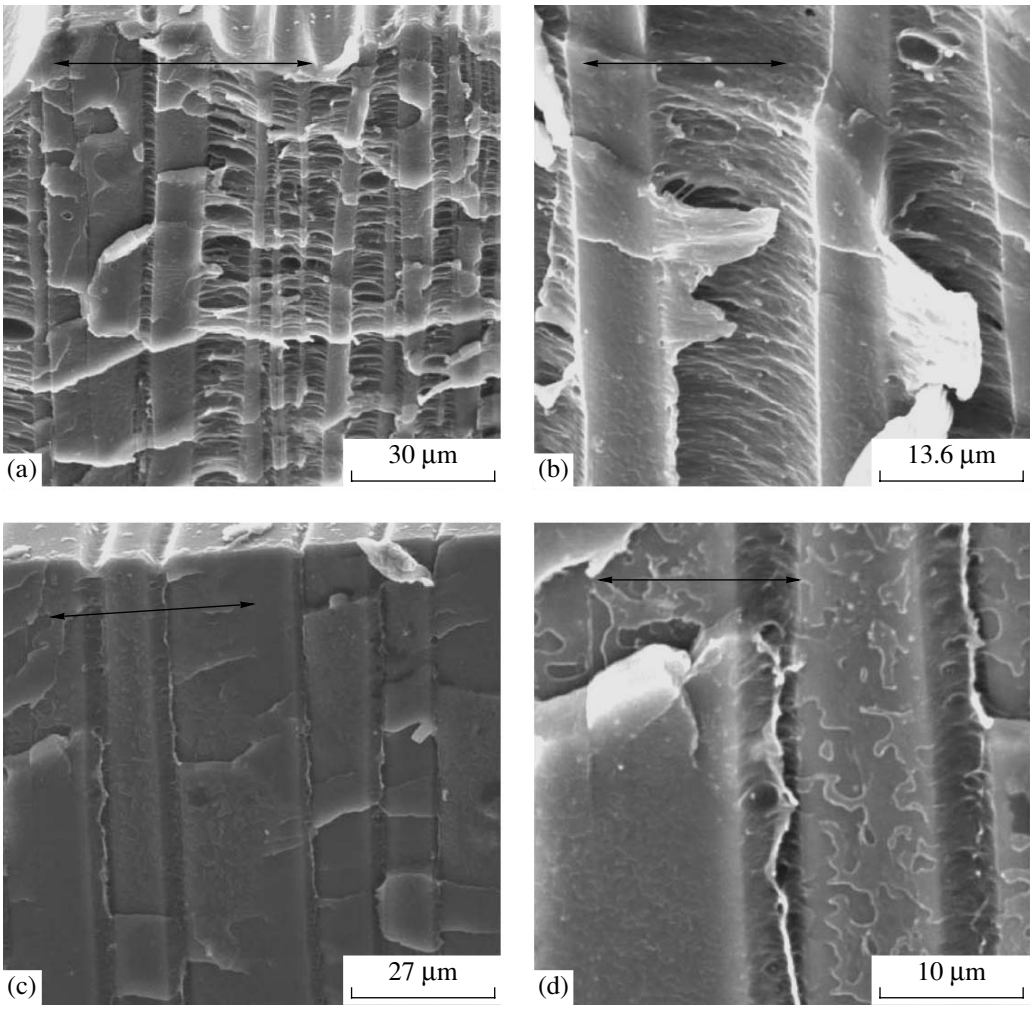

Fig. 8. SEM images of the solvent-crazed PET samples stretched in ethanol by 50%. Prior to tensile drawing, the samples were annealed at (a) 100, (b) 110, and (c, d) 140°C.

crazes, their typical fibrillar–porous structure is preserved.

As the annealing temperature is increased up to 110°C, structure of the solvent-crazed PET samples experiences dramatic changes (Fig. 8b). As in earlier cases, on the surface and in the volume of the sample, one can clearly see the crazes, which cross the entire cross section of the sample. However, a careful inspection allows one to distinguish certain structural changes in the structure of crazes. Electron microscopic examination makes it possible to observe that plastically deformed material, which is typical of crazes, contains less microvoids (cf. Figs. 3 and 8b).

Finally, preliminary annealing of PET at 140°C entails dramatic changes in the structure of the solvent-crazed samples. As follows from Fig. 8c, crazes in these samples have virtually equal and small widths. At high magnifications, one can distinguish that these crazes do not show their typical fibrillar–porous structure (Fig. 8d). In the volume of crazes, one can observe the regions of plastically deformed polymer that contain irregular and randomly located microvoids.

Let us now consider which structural changes are induced upon annealing. As was shown above, the surface of the test samples was decorated with a thin (10 nm) metallic coating. Figure 9 presents the structure of the samples after their annealing at 170°C. In the case of the preliminary annealing at 100°C, the solvent-crazed PET sample shows the SSE, but its intensity is much lower than that in the initial polymer sample without any annealing (Fig. 7). Nevertheless, as follows from Fig. 9a, preliminary annealing at 170°C leads to structural rearrangements that are typical of the SSE in PET. The surface of the fragments of bulk polymer between crazes appears to be covered with a regular wavy relief, and the surface of the films on the top of crazes is covered by a regular wavy relief with a small period and by the folds oriented in the perpendicular direction (Fig. 9b).

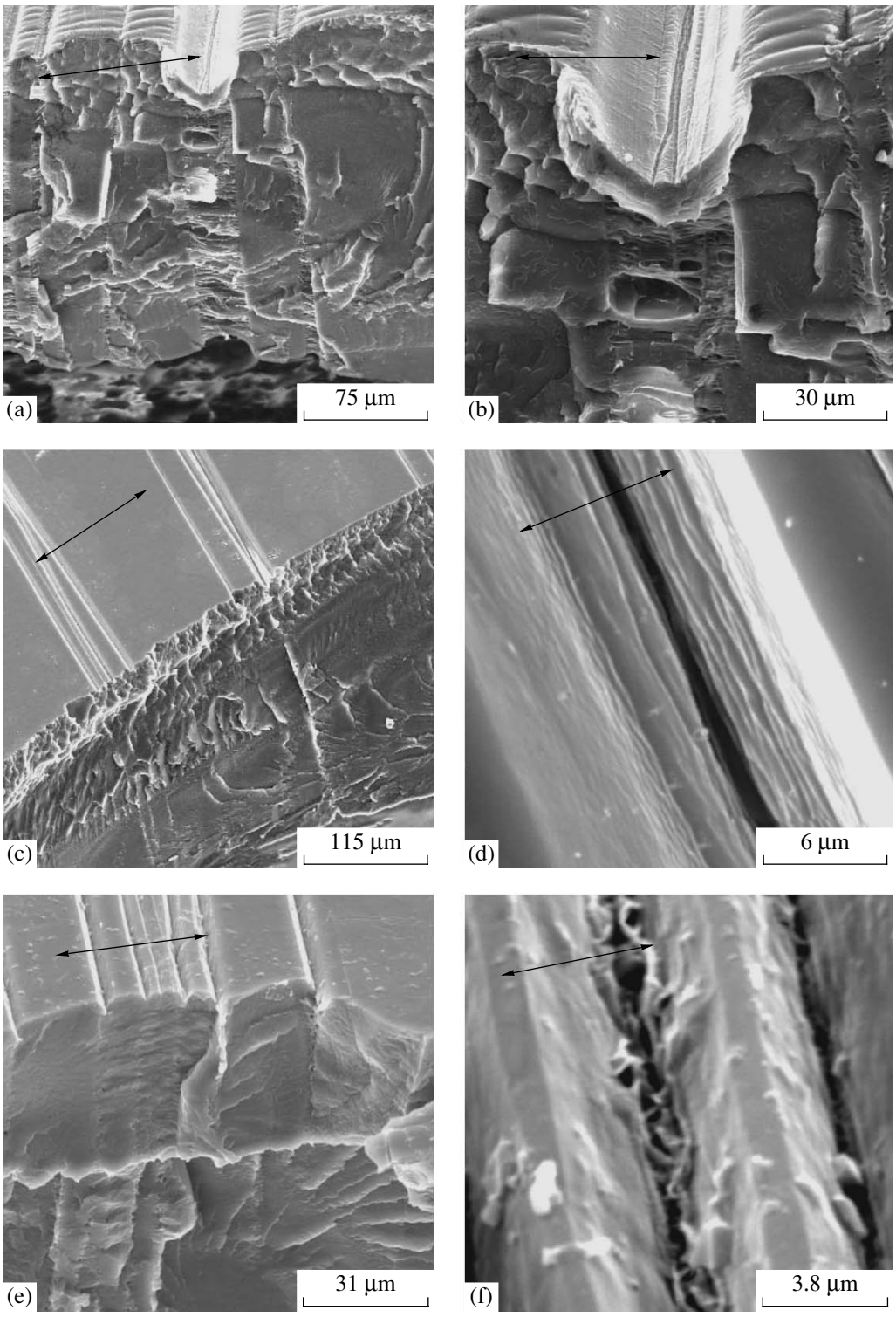

Fig. 9. SEM images of the solvent-crazed PET samples after their annealing at 170°C. Prior to tensile drawing, the samples were annealed at (a, b) 100, (c, d) 110, and (e, f) 140°C.

Preliminary annealing at 110°C likewise leads to marked structural changes in the solvent-crazed samples (Fig. 9c). In this case, the surface of the fragments of bulk polymer between crazes remains smooth; this observation indicates that the SSE phenomenon is fully suppressed. This conclusion agrees with the data presented in Fig. 7. At the same time, films on the top of crazes contain well-pronounced folds, which are devel-

oped in the coating during the contraction of the craze material (Fig. 9d).

Similar behavior is observed for the solvent-crazed PET samples after their preliminary annealing at 140°C. As in the former case, surface of the fragments of bulk polymer between crazes remains smooth (Fig. 9e), whereas the films on the top of crazes contain well-pronounced folds, which are directed along the axis of crazes (Fig. 9f).

Therefore, our experimental data fully support the above conclusion concerning the mechanism of structural rearrangements during annealing of the solvent-crazed PET samples. Preliminary crystallization of PET totally suppresses the occurrence of the SSE phenomenon; this result seems to be quite expected because SSE is based on the phenomenon of strain-induced crystallization. The above conclusions concerning the mechanism of structural rearrangements during the annealing of the solvent-crazed PET samples are based on direct microscopic data and demonstrare the advantages of the proposed visualization procedure [1–4].

REFERENCES

1. A. L. Volynskii, T. E. Grokhovskaya, A. S. Kechek'yan, et al., Dokl. Akad. Nauk **374**, 644 (2000).
2. A. L. Volynskii, A. S. Kechek'yan, T. E. Grokhovskaya, et al., Polymer Science, Ser. A **44**, 374 (2002) [Vysokomol. Soedin., Ser. A **44**, 615 (2002)].
3. A. L. Volynskii, T. E. Grokhovskaya, A. S. Kechek'yan, and N. F. Bakeev, Polymer Science, Ser. A **45**, 265 (2003) [Vysokomol. Soedin., Ser. A **45**, 449 (2003)].
4. A. L. Volynskii, T. E. Grokhovskaya, V. V. Lyulevich, et al., Polymer Science, Ser. A **46**, 130 (2004) [Vysokomol. Soedin., Ser. A **46**, 247 (2004)].
5. A. L. Volynskii, T. E. Grokhovskaya, A. I. Kulebyakina, et al., Polymer Science, Ser. A **48**, 527 (2006) [Vysokomol. Soedin., Ser. A **48**, 823 (2006)].
6. A. L. Volynskii, T. E. Grokhovskaya, O. V. Lebedeva, and N. F. Bakeev, Polymer Science, Ser. A **48**, 536 (2006) [Vysokomol. Soedin., Ser. A **48**, 834 (2006)].
7. A. L. Volynskii, T. E. Grokhovskaya, and N. F. Bakeev, Dokl. Akad. Nauk **400**, 487 (2005).
8. A. L. Volynskii, T. E. Grokhovskaya, V. I. Gerasimov, and N. F. Bakeev, Vysokomol. Soedin., Ser. A **18**, 201 (1976).
9. A. L. Volynskii, A. G. Aleskerov, T. E. Grokhovskaya, and N. F. Bakeev, Vysokomol. Soedin., Ser. A **18**, 2114 (1976).
10. A. L. Volynskii and N. F. Bakeev, *Highly Dispersed Oriented State of Polymers* (Khimiya, Moscow, 1984) [in Russian].
11. A. L. Volynskii and N. F. Bakeev, *Solvent Crazing of Polymers* (Elsevier, Amsterdam, 1995), p. 410.
12. A. L. Volynskii, S. L. Bazhenov, and N. F. Bakeev, Ross. Khim. Zh. **42** (3), 57 (1998).
13. A. L. Volynskii, S. L. Bazhenov, O. V. Lebedeva, and N. F. Bakeev, J. Mater. Sci. **35**, 547 (2000).
14. E. Passaglia, J. Phys. Chem. Solids **48**, 1075 (1987).
15. R. P. Kambour and R. W. Kopp, J. Polym. Sci., Part A-2 **7**, 183 (1969).
16. A. N. Gent and A. G. Thomas, J. Appl. Polym. Sci. **1**, 10 (1959).
17. R. P. Wool and K. M. Oconnor, Polym. Eng. Sci. **21**, 970 (1981).
18. A. S. M. Yang and E. J. Kramer, J. Polym. Sci., Part A: Polym. Chem. **23**, 1353 (1985).
19. J. A. Forrest and K. Dalnoki-Veress, Adv. Colloid Interface Sci. **94**, 167 (2001).
20. J. A. Forrest, Eur. Phys. J., E **8**, 261 (2002).
21. T. Kajiyama, K. Tanaka, N. Satomi, and A. Takahara, Sci. Technol. Adv. Mater. **1**, 31 (2000).
22. Y. M. Boiko and R. E. Prudhomme, Macromolecules **31**, 6620 (1998).
23. L. L. Berger and B. B. Sauer, Macromolecules **24**, 2096 (1991).
24. T. Kajiyama, K. Tanaka, and A. Takahara, Macromolecules **28**, 3482 (1995).
25. K. Tanaka, A. Takahara, and T. Kajiyama, Macromolecules **30**, 6626 (1997).
26. J. Hyun, D. E. Aspens, and J. J. Cuomo, Macromolecules **34**, 2396 (2001).
27. V. Busiko, P. Corradini, and F. Riva, Makromol. Chem., Rapid Commun. **1**, 423 (1980).
28. Yu. K. Godovskii, *Thermophysical Methods for Investigation of Polymers* (Khimiya, Moscow, 1976) [in Russian].
29. W. H. Smith and C. P. J. Sayior, J. Res. Natl. Bur. Stand. (U. S.) **21**, 257 (1938).
30. L. Mandelkern, D. E. Roberts, A. F. Diorio, and A. S. Posner, J. Am. Chem. Soc. **81**, 4148 (1959).
31. B. A. Fomenko, L. P. Perepechkin, B. V. Vasil'ev, and N. I. Naimark, Vysokomol. Soedin., Ser. A **11**, 1971 (1969).
32. H. J. Oswald, E. A. Turi, P. J. Harget, and Y. P. Khanna, J. Macromol. Sci., Phys. **13**, 231 (1977).
33. E. Liska, Kolloid Z. Z. Polym. **251**, 1028 (1973).
34. P. Pinnock and I. M. Ward, Trans. Faraday Soc. **62**, 308 (1966).
35. J. R. C. Pereira and R. S. Porter, Polymer **25**, 877 (1984).
36. D. E. J. Bosley, J. Polym. Sci., Part C: Polym. Lett. **20**, 77 (1967).
37. E. A. Sinevich, A. M. Prazdnichnyi, V. S. Tikhomirov, and N. F. Bakeev, Vysokomol. Soedin., Ser. A **31**, 1697 (1989).
38. E. A. Sinevich, A. M. Prazdnichnyi, and N. F. Bakeev, Vysokomol. Soedin., Ser. A **32**, 293 (1990).